SRTTU

Journal of Electrical and Computer Engineering Innovations

JECEI, Vol. 3, No. 2, 2015

Regular Paper

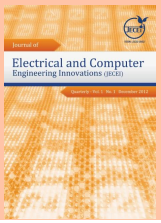

Optimal Design of Axial Flux Permanent Magnet Synchronous Motor for Electric Vehicle Applications Using GA and FEM

Mostafa Ahmadi Darmani[1], Hooman Hooshyar[1,*]

[1]Islamic Azad University, Science and Research Branch

[*]Corresponding Author's Information: hoomanhooshyar@gmail.com

ARTICLE INFO

ARTICLE HISTORY:
Received 8 November 2015
Revised 2 February 2016
Accepted 2 February 2016

KEYWORDS:
Axial Flux Permanent Magnet (AFPM)
Finite Element Analysis (FEA)
Genetic Algorithm (GA)
Torque Ripple Factor (TRF)
Electric Vehicles (EVs)

ABSTRACT

Axial Flux Permanent Magnet (AFPM) machines are attractive candidates for Electric Vehicles (EVs) applications due to their axial compact structure, high efficiency, high power and torque density. This paper presents general design characteristics of AFPM machines. Moreover, torque density of the machine which is selected as main objective function, is enhanced by using Genetic Algorithm (GA) and variation of PM characteristics, based on sizing equation and Finite Element Analysis (FEA). Moreover, torque ripple of the motor is reduced according to the effect of PM characteristics on Torque Ripple Factor (TRF). The designed machine produces sinusoidal back-EMF waveform. The results show that torque density is improved and the torque ripple is reduced. These results are validated by using 3D-FEA. Furthermore, to assess the obtained results by FEA method, an advanced vehicle simulator (ADVISOR) software is used to demonstrate the performance improvement over the Europe test drive cycles.

1. INTRODUCTION

Nowadays, electric vehicles are the best choice to reduce the air pollution caused by internal combustion cars. As shown in Fig.1, EVs have a coordinated system including battery, charger, propulsion (electric engine), body, control system, etc., its technology is interdisciplinary, a combination of power engineering, electronic engineering, mechanical engineering, etc. [1]. The part related to power engineers, is the designing and constructing the electric machines and its drive. The machine used in electric cars is ought to have fine structure, small, safe, with high power and torque density and high efficiency. Permanent magnet machines are a good choice for this case [2].

Permanent Magnet (PM) motors have gained increasing interests because of their high performance [3, 4]. They have several unique features such as high efficiency, high power and torque density, low rotor loss and small magnet thickness. AFPM machines can be single or double-sided or multistage, with or without armature slots/core. They have internal/external PM rotors, and contain a surface-mounted or interior PM. The double-sided AFPM motor is the most promising and widely used types. The topologies for the double-sided AFPM machines are the axial-flux one-stator–two-rotor (TORUS) and two-stator–one-rotor (AFIR) [3,4].The slotted AFIR motor has higher maximum torque density in smaller air-gap [5].

Therefore, the slotted AFIR AFPM motor is used in this study for modeling and simulation. The structure has two stators and one PM rotor disc. The accurate analysis of the torque for the given motor dimensions, 3D-finite element analysis (3D-FEA) is helpful.

This study uses GA-based sizing equation and sensitivity analysis of PM characteristic with

performance analysis conducted via FEA in the design process of an optimal AFPM machine. The presented design is a slotted AFIR AFPM synchronous machine. The design optimization of a 20 kW, three-phase, 2400 rpm, and 10 poles AFPM synchronous motor is based on the practical limitations for a typical electric vehicle. The design objectives are considered as maximum torque density, less torque ripple, and minimum total harmonic distortion (THD) of the induced EMF. The various characteristics of the designed motor are then obtained through electromagnetic field analysis using FEA software. Various characteristics of the PMs are also investigated to get the most sinusoidal back-EMF and reduced torque ripple. In order to validate the design, the performance of the designed AFPM synchronous machine is simulated. It is found from the results that the optimized machine exhibits low torque ripple, high-torque density, low THD of the induced voltage verifying the analytical results based on FEA and sizing equation. So, the optimized motor has a better characteristic in propulsion system based on ADVISOR software.

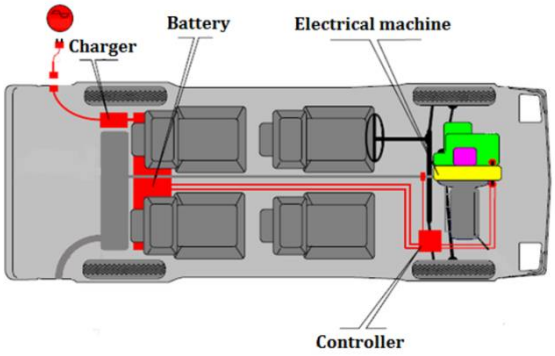

Figure 1: Electric vehicle schematic.

In this paper, the sizing equations needed for AFPM design are presented in Section 2. General design considerations and limitations for axial flux permanent magnet motors are introduced in Section 3. Some aspects of genetic algorithm are introduced in Section 4. In Section 5, improved design of an AFPM is validated by 3D finite element analysis. Torque ripple reduction, optimization and final design results are given in Section 6. In Section 7, optimization AFPM is tested in ADVISOR software. Finally, conclusions are given in section 8.

2. SIZING EQUATION

The main dimensions of each electrical machine are determined by its output power equation. Assuming negligible leakage inductance and resistance, the machine output power is expressed as [6, 7, 8]:

$$P_{out} = \eta \frac{m}{T} \int_0^T e(t).i(t)dt = mK_p \eta E_{pk} I_{pk} \quad (1)$$

where e(t) is the phase of air-gap EMF, i(t) is the phase current, η is the machine efficiency, m is the number of phases, and T is the period of one EMF cycle. E_{pk} and I_{pk} are peaks of phase of air-gap EMF and current, respectively. $K_p$is electrical power waveform factor, defined as:

$$K_p = \frac{1}{T} \int_0^T \frac{e(t) \times i(t)}{E_{pk} \times I_{pk}} dt = \frac{1}{T} \int_0^T f_e(t).f_i(t)dt \quad (2)$$

where$f_e(t) = e(t)/E_{pk}$ and $f_i(t) = i(t)/I_{pk}$ are the expressions to normalize EMF and current waveforms. The current waveform factor (K_i) for the current effect is defined as:

$$K_i = \frac{I_{pk}}{I_{rms}} = \frac{1}{\sqrt{\frac{1}{T}\int_0^T (\frac{i(t)}{I_{pk}})^2 dt}} \quad (3)$$

Here I_{rms} is the root mean square (rms) of the phase current.

The peak value of the phaseair-gap of EMF for the AFPM machine in (1) is expressed as:

$$E_{pk} = K_e N_{ph} B_g \frac{f}{p} (1 - \lambda^2) D_o^2 \quad (4)$$

K_e is the EMF factor that incorporates the winding distribution factor (K_w) and per-unit portion of the air-gap area covered by the salient poles of the machine (if any);N_{ph} is the number of winding turns per phase; $B_g$is the flux density in the air gap; f is the converter frequency; p is the machine pole pairs; λ is the diameter ratio equal to D_i/D_o whichD_O is the outer surface diameter and D_i is the inner surface diameter of the AFPM machine. The peak phase current for (1) is expressed as:

$$I_{pk} = A\pi K_i \frac{1+\lambda}{2} \cdot \frac{D_o}{2m_1 N_{ph}} \quad (5)$$

wherem_1 is the number of phases, and A is the total electrical loading. The sizing equation for AFPM machines is presented as:

$$P_{out} = \frac{1}{1+k_\phi} \frac{m}{m_1} \frac{\pi}{2} K_e K_i K_p K_L A B_g \eta \frac{f}{p} \times (1-\lambda^2)(\frac{1+\lambda}{2}) D_o^3 \quad (6)$$

$k_\phi$is the electrical loading ratio on the rotor and stator;and K_L is the aspect ratio coefficient of a specific machine structure that considers the consequence of loss, temperature rise, and design efficiency requirements. The machine torque density for the total volume is defined as:

$$T_{den} = \frac{P_{out}}{\omega_m \frac{\pi}{4} D_{tot}^2 L_{tot}} \quad (7)$$

whereD_{tot} and $L_{tot}$are the machine's total outer diameter and total length, respectively, including the outer diameter and endwinding protrusion of the

stack from the radial and axial iron stacks. ω_m is rotor angular speed [9].

3. CONSIDERATIONS AND LIMITATIONS

Volvo 3P is interested in electrical wheel motors for trucks in long-haul applications and financed a feasibility study, during 2008-2009. An initial study to investigate the potential performance improvement and a rough evaluation of the available space inside the rim was carried out by Volvo technology [10]. Table 1 lists the machine geometry restrictions by Volvo technology. Also, consideration and limitation of the proposed motor that are based on the typical AFPM motor are given in Table 1 [10, 11].

TABLE 1
DESIGN GEOMETRY

Geometry Restrictions	
Motor outer diameter (D_o)	$D_o \leq 260\ mm$
Motor length (L_{tot})	$L_{tot} \leq 72.5\ mm$
Limitations	
Diameter ratio (λ)	$0.4 \leq \lambda \leq 0.7$
Air-gap length (g)	$0.5 \leq g \leq 1.5$
Air-gap flux density(B_g)	$0.35 \leq B_g \leq 0.95$
Electrical loading (A)	$30000 \leq A \leq 35000$
Requirement	
Rated output power	20 kW
Rated speed	2400 rpm
Number of pole pairs, p	10
Number of phases, m	3

According to sizing equation and consideration of the minimum values of Table 1, primary dimensions of motor calculated and are listed in Table 2.

TABLE 2
DIMENSIONS OF PRIMARY MOTOR

Design Parameters	Value
Rated output power	20 kW
Rated speed	2400 rpm
Number of poles, $2p$	10
Number of stator slots	48
Outer diameter, D_o	260 mm
Inner diameter, D_i	166.4 mm
Diameter ratio, λ	0.64
Air-gap length, g	1 mm
Rotor core length, L_{cr}	10.1 mm
Stator core length, L_s	26.8 mm
Motor length, L_{tot}	72.5 mm
Permanent magnet length, L_{pm}	3.4 mm
Pole arc embrace	0.7

4. GENETIC ALGORITHM

To transform constrained optimization problem into unconstrained one, the penalty function method is used. In this method, the penalty term replaces a constraint optimization problem with a series of unconstrained problems, in such a way that the solutions converge to the solution of the original constrained problem. Genetic Algorithm is a computational model inspired by evolution. This algorithm encodes a potential solution to a specific problem on a simple chromosome like data structure and applies recombination operators to these structures, to preserve critical information. Genetic algorithm is often viewed as function optimizer. The range of problems to which genetic algorithmhasbeen applied is quite broad [12, 13].

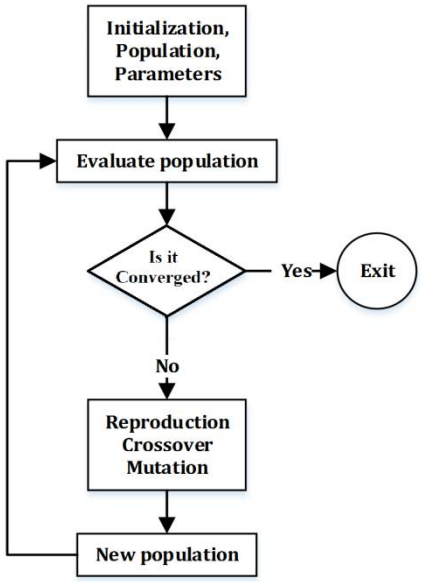

Figure 2: Flowchart of GA optimization.

It should be noted that the GA differs substantially from many of traditional search and optimization methods. The four most significant differences are as follow [12, 13]:

- GAsearchesa population of points in parallel, not a single point.
- GA does not require derivative information or other auxiliary knowledge; only the objective function and corresponding fitness levels influence the directions of the search.
- GA uses probabilistic transition rules, not deterministic ones.
- GA works on an encoding of the parameter set rather than the parameter set itself (except where real-valued individuals are used).

A design should include a maximum torque density incorporating and maintaining within the design restrictions and requirements. Optimization of the AFPM with the highest possible torque density using GA is shown in Fig. 2. In this study, stator outer diameter, diameter ratio,maximum air-gap fluxdensity and electric loading areselected as

chromosomes.Therestrictions used in the design procedure are machine outer diameter and also the length of the machine. Chromosomes evolve from each generation via successive iterations, with every generation evaluated by a fitness measure. In this case, half of all genes are chosen to produce a new generation and the other half is ignored. The AFPM machine torque density (7) is chosen as the fitness function, and is calculated for each step and chromosome.

The MATLAB-programming fitness function variation for the 50 generations is illustrated in Fig. 3. The best fitness of GA is shown about 0.22. The dimensions of the motor, with the highest torque density through GA optimization are given in Table3.

TABLE 3
DIMENSIONS OF THE MOTOR, WITH THE HIGHEST TORQUE DENSITY OBTAINED VIA GA

	T_{den} W/m^3	T N.m	B_g	A A/m	λ	D_o mm	g mm	L_{pm} mm	L_{cs} mm	L_{cr} mm	D_{ss} Mm	L_{tot} mm
1	0.022	98.1	0.95	33843	0.55	260	0.95	3.4	10.2	10.5	15.8	71.2
2	0.022	92	0.94	34995	0.504	252	0.91	3.6	10.2	11.1	13.7	67.9
3	0.022	90	0.906	33704	0.505	257	0.98	3.4	10.1	9.4	14.1	66.5
4	0.021	94	0.936	34119	0.501	256	0.92	3.5	10.3	11	15.1	70.9
5	0.021	98.14	0.945	33454	0.453	258	0.9	3.6	10.2	11.3	16.3	73.2
6	0.021	92.45	0.949	33987	0.504	254	0.9	3.6	10.4	11.8	15.4	72.4
7	0.020	95.3	0.94	33397	0.503	259	0.91	3.6	10.5	11.4	16.6	74.6
8	0.020	96.3	0.94	33435	0.503	258	0.91	3.6	10.5	11.4	16.3	73.9
9	0.019	90	0.946	31753	0.468	256	0.9	3.6	10.2	11.4	17.1	74.9
10	0.019	96.68	0.95	33023	0.5	260	0.89	3.6	10.6	12.1	17.6	77.6

5. FINITE ELEMENT ANALYSIS

GA maximizes the torque density of AFPM machine. 3D FEA is the powerful method to analyze magnetic circuit and torque density of the double-sided AFIR AFPM motor [14].

In each side of rotor disc, ten axially magnetized Nd–Fe–B PMs are mounted on the surface of rotor disc facing the two stators.The optimized winding configurations of the AFPM motor, simulated in this study, are shown in the appendix. The designed motor is shown in Fig. 4. The design was simulated with ANSYS Maxwell 3D 15 software.

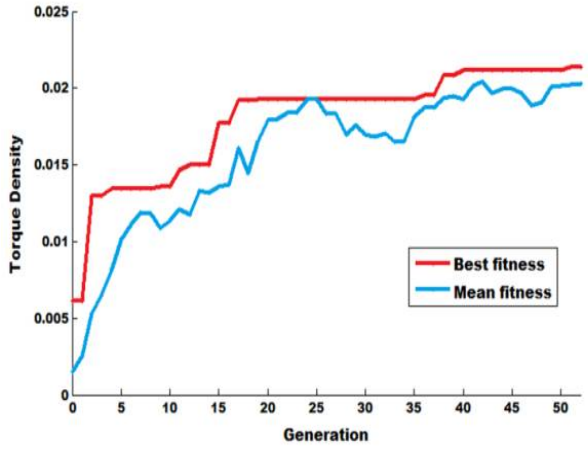

Figure 3: Fitness function variation during GA optimization.

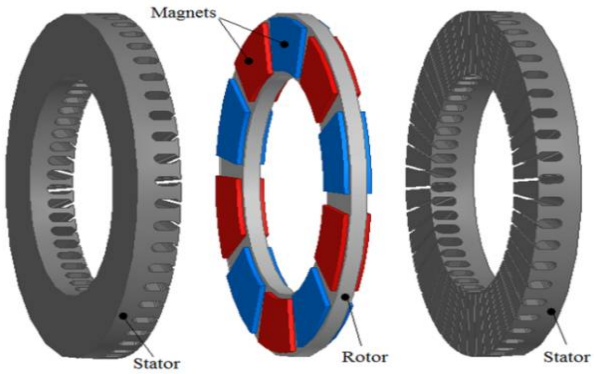

Figure 4: AFIR AFPM motor structure.

From the symmetric construction, only 1/4 of the machine has been modeled. The flux density distribution in1/4 of the motor used is illustrated in Fig. 5.

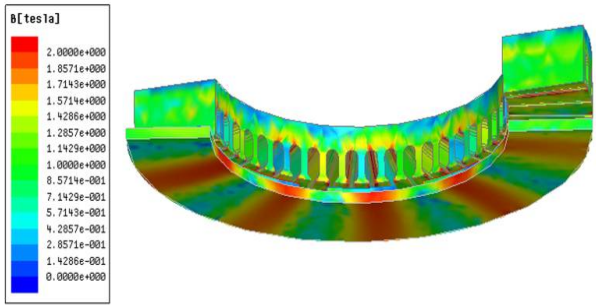

Figure 5: Flux-density plot.

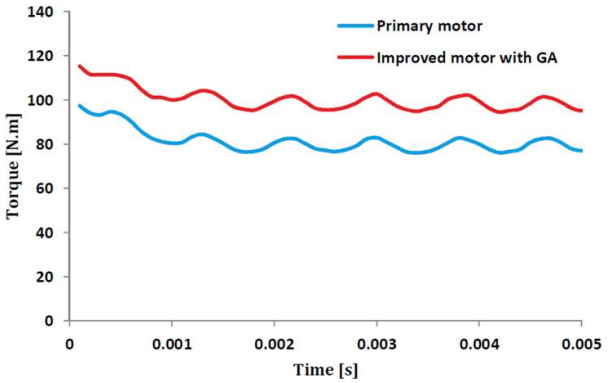

Figure 6: Average torques in primary and improved cases of motor

Primary motor and improved motor with GA has been simulated and the results are compared in Fig. 6. As it is seen in the figure, the average Torque has increased from 79.21 to 98.06.

6. Last Optimization and Final Design

The average torque has been maximized in the previous section, but another characteristic thatshould be improved is torque ripple.

In ideal case, if the back EMFs and the armature phase currents are sinusoidal, the electromagnetic torque will be constant and no torque ripple exists.

Induced phase back EMFs are not sinusoidal and contain high-order harmonics, because, almost all practical stator windings and PM field distributions have some significant winding and flux density harmonics.

Many techniques such as using appropriate stator winding type, skewing either stator slots or rotor magnets, rotor shifts, and magnet skewing are used to achieve this goal from a machine design perspective. The optimized winding configuration for a reduced torque ripple is explained in the appendix.

The other goal for reduced torque ripple is sensitivity analysis of magnet characteristics. Besides, minimizing the torque ripple reduces the value of the average torque.

For solving this problem, the Torque Ripple Factor (TRF) is defined as the ratio of torque ripple to average torque and expressed as Fig. 17.

The TRF is investigated for different magnet skew angles and pole arc ratios. After this procedure, the optimum design point is obtained for minimum TRF. In this case it is supposed that the average torque does not reduce below 90 N.m.

The optimum skew angle is shown clearly in Fig. 7. A summary of the results for different skew angles is provided in Table4.

As shown in Fig. 7, increasing skew angle improves TRF. For 9 degree skew angle, average torque becomes lower than 90 N.m which is not acceptable.

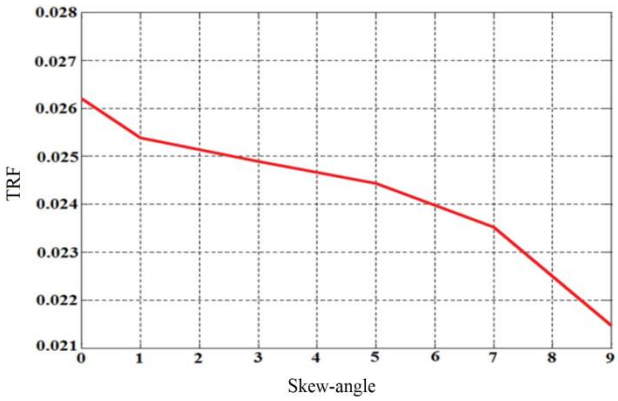

Figure 7: TRF of the motor as a function of magnet skew angle.

Table 4
TRF Results for Different Skew Angles

	0	1	3	5	7	9
T	98.1	97.7	94.81	92.02	90.12	88.51
Ripple	2.57	2.48	2.36	2.25	2.12	1.9
TRF	0.0262	0.0254	0.0249	0.0244	0.0235	0.0215

The optimum skew angle and magnet pole arc ratio are shown in Fig. 8. As shown in this figure, TRF is improved by maximizing pole arc ratio around 0.8. After that TRF will be increased.

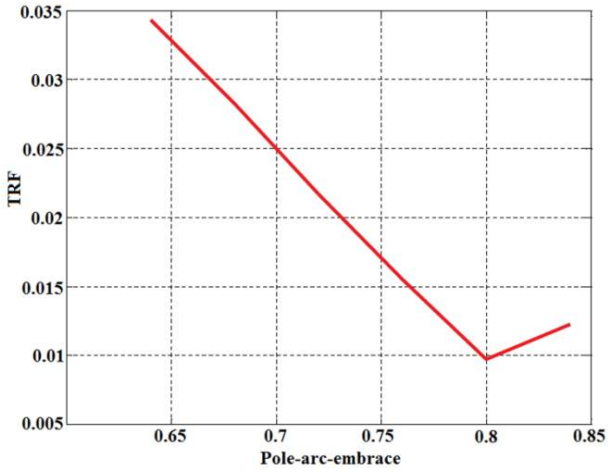

Figure 8: TRF of the motor as a function of PM pole arc ratios.

The results for different PM pole arc ratios are provided in Tables 5.

Table 5
TRF Results for Different PM Pole arc Ratios

	0.64	0.68	0.72	0.76	0.8	0.84
T	93.5	96.28	99.55	101.92	102.96	104.42
Ripple	3.21	2.72	2.16	1.58	1	1.28
TRF	0.0343	0.0283	0.0217	0.0155	0.0097	0.0123

According to Figures 7,8 and Tables 4,5, torque ripple is very sensitive to PM pole arc ratio and skew angle, and precision of these parameters is very important for smooth-torque PM motors.

Fig. 9 shows the TRF plot as a function of magnet pole arc ratio and magnet skew angle. It is clear from the figure that the minimum value of TRF occurs near a PM pole arc ratio of 0.8 and a skew angle of 7.

AFPM motor is simulated for new values. The torque ripple comparison between final design and primary design is shown in Fig. 10.

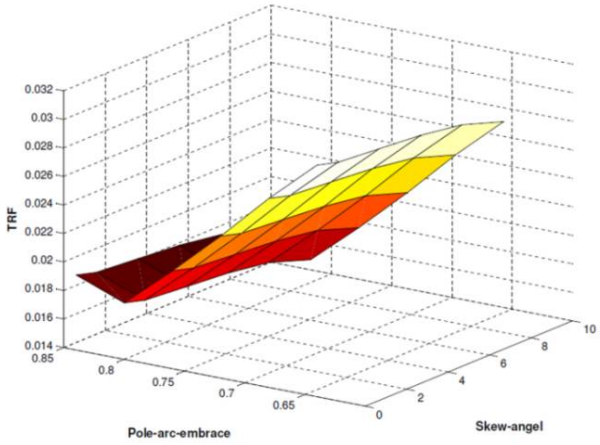

Figure 9: TRF of AFPM machine as a function of pole arc and magnet skew angle.

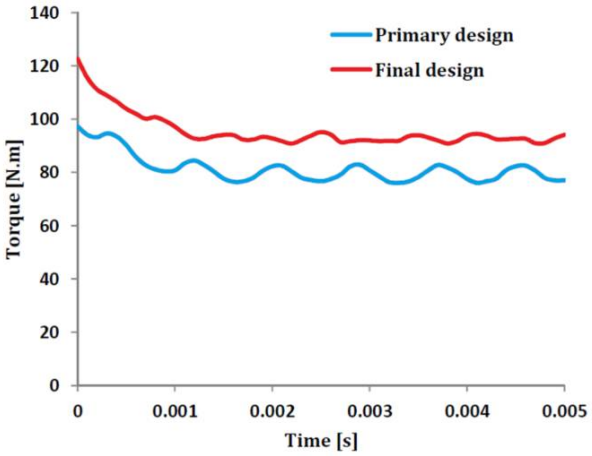

Figure 10: Comparison of torque in priamary and final designs.

For better comparison, back-EMF waveform and harmonics are shown in Fig.11 and Fig. 12.

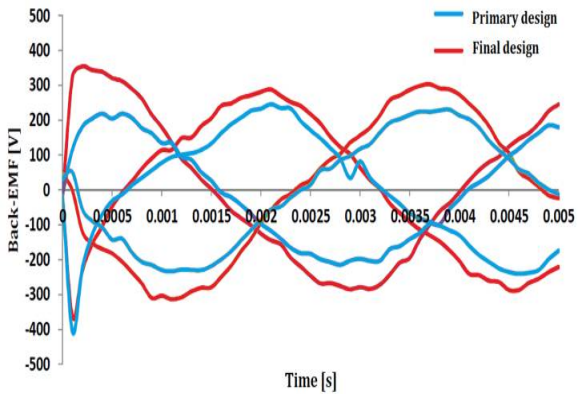

Figure 11: Comparison of Back-EMF waveform in priamary and final designs.

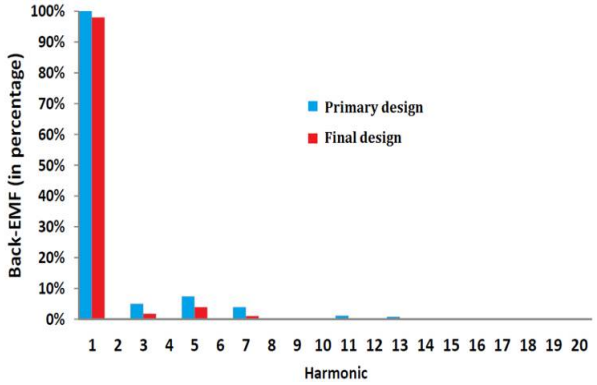

Figure 12: Comparison of harmonic components for the primary and final designs.

As it is shown in Fig. 10, the average torque is maximized from 79.21 to 92.53 and torque ripple reduced from 2.89 in primary design to 1.12 in final case to prove correctness of optimization process. Finally, the average torque increased about 23% and torque ripple reduced about 61%. Table 6 lists the final design dimensions and specifications of the machine.

TABLE 6
FINAL DESIGN RESULT OF AFPM

Design data	Value
Outer diameter, D_o	260 mm
Inner diameter, D_i	143 mm
Diameter ratio, λ	0.55
Air-gap length, g	0.95
Rotor core length, L_{cr}	10.5
Stator core length, L_{cs}	10.2
Stator-slot depth,d_{ss}	15.8
Motor length, L_{tot}	71.2
Permanent magnet length, L_{pm}	3.4
Rated output power	20 kW
Rated speed	2400 rpm
Number of poles, 2*p*	10
Number of stator slots	48
Frequency	200 Hz
Efficiency	90 %

7. COMPARISON OF THE PRIMARY AND FINAL DESIGNSIN PROPULSION SOFTWARE

It is known that the size of electric vehicles is a major problem. It is due to difficulty of storing the electrical energy.Anyway, this is certainly a critical issue in the design of any electric vehicle. The cycles are intended to correspond to realistic driving patterns in different conditions.During these simulations, the vehicle speed is supposed to change constantly, and thus the performance of all the other parts of the system is also variable, which makes the computations more complex [15]. Aparticular rule is the ECE-15 drive cycle, shown in Figure 13, which is useful for testing the performance of small vehicles

such as battery electric cars.

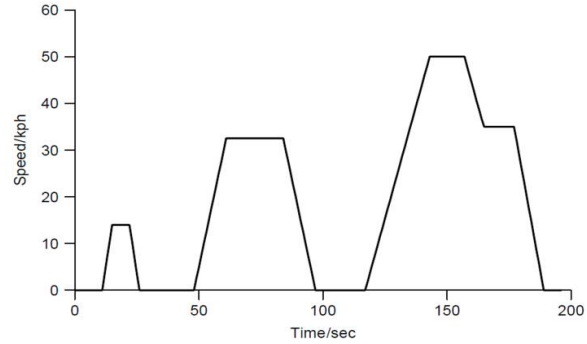

Figure 13: European urban driving schedule ECE-15.

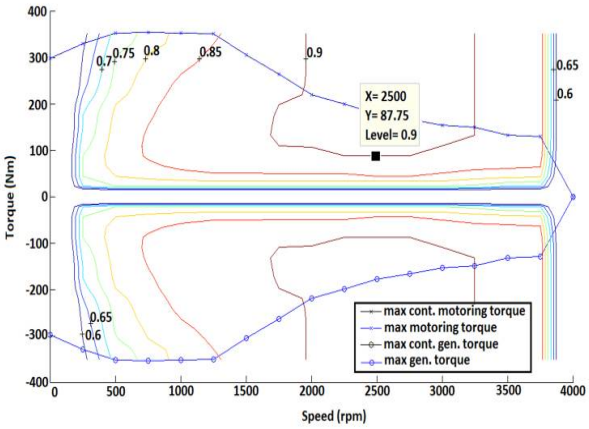

Figure 14: Torque-speed characteristic of motor

From the vehicle data and performancerequirements, torque speed characteristic of motor is shown in Fig. 14.

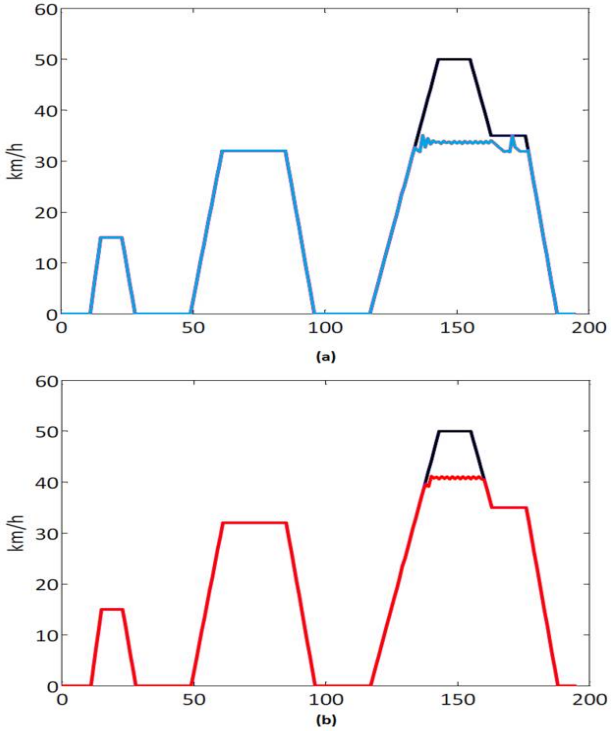

Figure 15: Amount of coverage of selected drive cycle.
a) Primary motor, b) Final motor

As it shown in Fig. 14, for speed of 2400 rpm, if the motor has torque over 87 N.m, the efficiency becomes 90%. For better comparison, primary and final designs are simulated in advanced vehicle simulator (ADVISOR) software [16].

The amount of coverage of selected drive cycle is shown in Fig. 15. As shown, the final motor coveres more parts of the cycle than the primary motor.

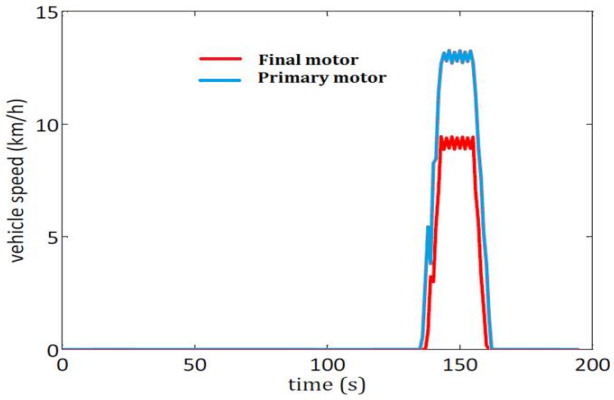

Figure 16: Vehicle speeds for primary and final motors.

In Fig. 16, differences between request and achieved speed of primary and final designs are shown. The final motor covers more amount of requested speed than the primary motor. Besides, lack of request speed is less in the final motor than the primary one. In Fig. 17, the power loss of motor is shown. The temperature of the final motor is lower than that of the primary one as shown in Fig. 18.

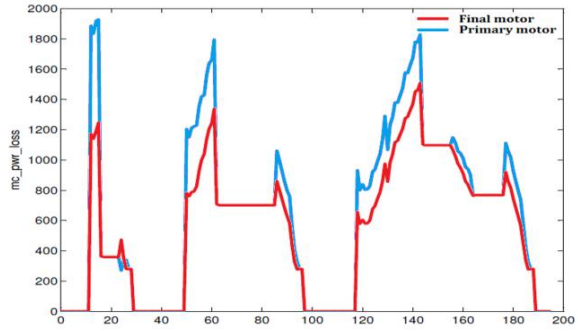

Figure 17: Motor power loss in primary and final motors.

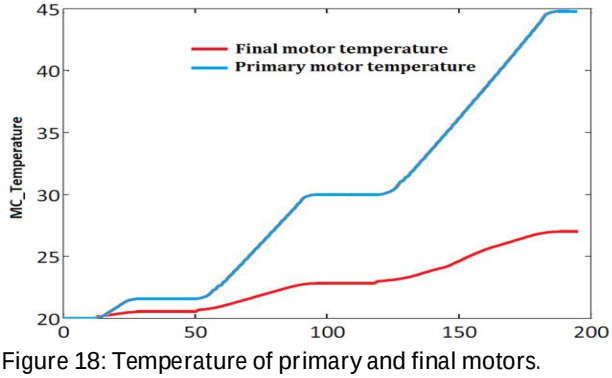

Figure 18: Temperature of primary and final motors.

8. CONCLUSIONS

In this paper, AFPM is designed for using in EVs. Genetic algorithm and sensitivity analysis are presented for motor optimization.

The results of the optimization by the FEA have confirmed that the proposed method, improves the characteristics of AFPM motor.

The final and the primary motors have been compared with the advanced vehicle simulator software.It was shown that the final motor with improved average torque has more advantages than the primary one for using in transportation application.

Torque ripple, especially at low speeds, is undesirable for vehicle applications [17]. Therefore, it is necessary to minimize torque ripple particularly in the low speed operation of the vehicle. So, in final motor design, the torque ripple was reduced which shows another benefit of mentioned motor in EVs applications.

APPENDIX

A particular method has been used to position the coils [9].

Many possibilities exist for pole and slot number combinations similarto windings layouts. Assumptions are also necessary to identify desirable windings.

Due to the large number of poles for motor, fractional-slot winding are selected. However, based on the fact of symmetry, the number of slots can be divided by number of phases (=3).

The benefits of fractional slot windings arereducing the high frequency harmonics of MMF and EMF waveforms and having more choices in choosing coil pitch.

For example, a 48 slot, 10 poles machine, has $4\frac{4}{5}$ slot per pole, and can be selected 3 or 4 for coil pitch (always smaller than slot per pole), supposing that S is the number of slots and P is the number of poles. So, the number of slots per pole per phase is $\frac{S/_3}{p}$.

If k is the biggest common divisor between $S/_3$ and p, the number of slots per pole per phase can be written as:

$$\frac{S/_3}{p} = \frac{k.S_k}{k.p_K} = \frac{S_k}{p_K} \quad (8)$$

$\frac{S_k}{p_K}$is the aspect ratio of fractional slot winding. k represents the number of windings that can be repeated. Also, k represents the number of possible paths.

$$\frac{S_k}{p_K} = \frac{48/_3}{10} = \frac{16}{10} = \frac{2\times 8}{2\times 5} = \frac{8}{5} \quad (9)$$

Here the biggest common divisor is k=2. So, number of windings that can be repeated or number of possible paths is 2. Aspect ratio $\frac{8}{5}$ shows that 8 coils belonging to each phase can be distributed under 5 neighbor poles. Table 7 illustrates a simple grouping of winding. Slot pitch calculated based on the electrical angle is:

$$\gamma = \frac{18\times p}{S} = \frac{180\times 10}{48} = 37\frac{1}{2}^{\circ} \quad (10)$$

Phase grouping presented as

Phase A: $0 \le A \le 60°$

Phase B: $60° \le B \le 120°$

Phase C: $120° \le C \le 180°$

TABLE 7
DISTRIBUTED WINDING IN 24 SLOTS

Pole pitch 1					
Slot number	1	2	3	4	5
Angle	0	37.5	75	112.5	150
Phase	A	A	-C	-C	B
Pole pitch 2					
Slot number	6	7	8	9	10
Angle	7.5	45	82.5	112	157.5
Phase	-A	-A	C	-B	-B
Pole pitch 3					
Slot number	11	12	13	14	15
Angle	15	52.5	90	127.5	165
Phase	A	A	-C	B	B
Pole pitch 4					
Slot number	16	17	18	19	20
Angle	22.5	60	97.5	135	172.5
Phase	-A	C	C	-B	-B
Pole pitch 5					
Slot number	21	22	23	24	
Angle	30	67.5	105	142.5	
Phase	A	-C	-C	B	

It should be mentioned that the sequence of phase groups is A, -C, B, -A, C, -B. Distributed winding in 24 slots is shown in Fig. 19.

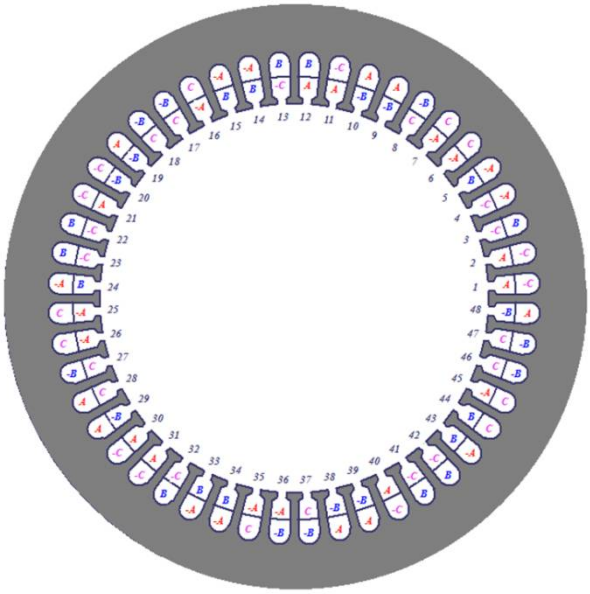

Figure 19: Distributed winding in 24 slots

REFERENCES

[1] M. J. Yang, H. L. Jhou, B. Y. Ma, K. Kai Shyu,"A Cost-Effective Method of Electric Brake With Energy Regeneration for Electric Vehicle" *IEEE Trans. Ind. Electron*.,vol. 56, no. 6, pp. 2203-2212, June. 2009.

[2] G. Nanda, N. C. Kar, "A Survey And Comparison Of Characteristics Of Motor Drives Used In Electric Vehicles" *IEEE Electrical and Computer Engineering Conf*, pp. 811-814.

[3] S. Onoda, A. Emadi,"PSIM-Based Modeling of Automotive Power Systems Conventional, Electric, and Hybrid Electric Vehicle" *IEEE Trans.Vehicular Technology*, vol. 53, no. 2, pp. 390-400, Mar. 2004.

[4] Aydin, M., S. Huang, T.A. Lipo, "Axial Flux Permanent Magnet Disc Machines: A Review" *Research Report*,2004-2010.

[5] S. AsgharGholamian, M.T. AbbasiAblouie, A. Mohseni and S. EsmaeiliJafarabadi, "Effect of Air Gap on Torque Density for Double-Sided Axial Flux Slotted Permanent Magnet Motors using Analytic and FEM Evaluation", *Journal of Applied Sciences Research*, 5(9): 1230-1238, 2009.

[6] J. Gieras, Rong-Jiewang and J.Kamper, "Axial Flux Permanent Magnet Brushless Machines", Publisher:Springer,2005.

[7] D.C. Hanselman, "Brushless Permanent-magnet Motor Design", Number 2, McGraw-Hill,Inc, 1994.

[8] Funda. Sahin,"Design and development of high speed axial-flux permanent magnet machines" Thesis, Doctor of Philosophy,Cip-Data ClibraryTechnischeUniversiteit Eindhoven,2001.

[9] Qu Ronghai, T.A. Lipo, "Analysis and modeling of air-gap and zigzag leakage fluxes in a surface-mounted permanent-magnet," Machine IEEE Transactions on Industry Applications, Volume 40, Issue 1, pp 121-127, 2004

[10] Cirani M. &Lindstr¨om J. "Electric hub wheel motors: An initial studyfor long haul applications" *Technical report*, Volvo 3P, 2009.

[11] Chiristian Du-Bar, "Design of an axial flux machine for an in-wheel motor application" Master of science thesis, Department of Energy and Environment, *Chalmers University Of Technology*, 2011.

[12] S.Rao.Singiresu, "Engineering Optimization:Theory and Practive", 3rd Edition,Wiley Eastern,1996.

[13] S.S.Roa,"Optimization Theory and Application", Wiley Eastern Ltd, New Dehli,1985.

[14] N. Bianchi, Electrical Machine Analysis using Finite Element. BocaRaton, FL, USA: Taylor & Francis/CRC Press, 2005.

BIOGRAPHIES

Mostafa Ahmadi Darmani was born in Tehran, Iran, in 1987. He received his M.Sc. degree in power electrical engineering from Islamic Azad University, Science and research branch, Tehran, Iran, in 2014.

He is currently working in Islamic Azad University Tehran, South branch as a lecturer. His research interests include design, modeling, control and finite-element analysis of electrical machines, electromagnetic devices and renewable energy system.

HoomanHooshyar was born in Tehran, Iran, in 1986. He received his M.Sc. degree in power electrical engineering from Islamic Azad University, Science and Research branch, Tabriz, Iran, in 2014.

His research interests include design, modeling, control and finite-element analysis of electrical machines, wind turbines and electric vehicles.